ELSEVIER

Journal of Structural Geology 27 (2005) 1721–1739

JOURNAL OF STRUCTURAL GEOLOGY

www.elsevier.com/locate/jsg

Architecture of normal faults in the rift zone of central north Iceland

Tatiana Tentler[a,*], Stefano Mazzoli[b]

[a]*Department of Earth Sciences, University of Uppsala, Sweden*
[b]*Dipartimento di Scienze della Terra, Università di Napoli 'Federico II', Italy*

Received 10 March 2004; received in revised form 3 April 2005; accepted 5 May 2005
Available online 8 August 2005

Abstract

This work examines the architecture and propagation of normal faults that accommodate extension in the rift zone of central north Iceland. It is based on a structural study of portions of three grabens, their normal faults and dilational fractures in basaltic lavas of the Fremri-Namur and Dyngjufjöl volcanic systems. We analyzed the shape, throw and dilation along faults in order to infer their possible evolution. The shape of throw profiles departs from elliptical varying along each fault with throw being lower at the fault and segment tips. Propagation of fault segments is accommodated by dilational fractures nucleating at their respective tips. Segments link by lateral propagation of one or both tips or by the development of intervening linking segments. Two orders of fault segmentation indicate that the present throw accumulated by many increments as the fault scarps changed their geometries. Faults have large dilational components weakly correlated with fault throw and length.

Keywords: Normal fault; Throw; Dilation; Fault segmentation; Fault propagation

1. Introduction

Regions of active extension are commonly associated with normal faulting and dilational fracturing in the upper crust. The orientation of a fault zone depends mainly on the bulk regional stress field and local stress perturbations across the plate boundaries as shown by fault slip analyses (Bergerat et al., 1990; Angelier et al., 1997) and monitored by GPS measurements (Foulger et al., 1992; Sigmundsson et al., 1995), while the location of individual fractures is also controlled by the mechanical characteristics of the faulted material (Pollard et al., 1982; Cowie, 1998). Normal faults typically consist of offset linked segments with displacement along them being controlled by a number of factors. Among them are those characterizing the local fault surface: its shape, aspect ratio, and the frictional properties along it (Maerten et al., 1999; Mazzoli and Di Bucci, 2003), variations in lithology and mechanical rock properties (Cartwright et al., 1995; Wilkins and Gross, 2002), fault location (Dawers et al., 1993; Ackermann et al., 2001) and configuration of stress field (Acocella et al., 2000; Gudmundsson, 2000). Analytical modeling (Walsh and Watterson, 1987; Walsh et al., 2002) and 3-D boundary element modeling (Willemse, 1997; Maerten et al., 1999) suggest that normal faults grow episodically with displacement accumulating through stages. As fault segments propagate towards each other, areas around their overlaps serve as sites of local fracturing where segment linkage is governed by the stress state at their tips (Cartwright et al., 1995; Cowie, 1998).

This study examines the architecture of brittle extensional fractures in a rift zone of Iceland. Analysis of the shape of fault scarps and distribution of throw are important for better understanding of the mechanics of fault growth, the evolution of the fault population, and the general systematics of brittle failure. Here we analyze the shape, throw and width of grabens within a spreading zone of Iceland in order to infer the evolution of fault propagation.

Iceland represents a rare example of an emergent portion of a divergent plate boundary where structures that are usually submarine can be observed conveniently on land. The good exposure of faulted blocks in Iceland, the relatively simple succession of mostly basaltic lavas and hyaloclastites, and a highly homogeneous extension offer the opportunity to study fault growth in comparatively

* Corresponding author. Tel.: +46 18 4712569; fax: +46 18 4712591.
E-mail address: tatiana_tentler@hotmail.com (T. Tentler).

0191-8141/$ - see front matter © 2005 Elsevier Ltd. All rights reserved.
doi:10.1016/j.jsg.2005.05.018

simple form. The processes common at oceanic ridges are complicated in Iceland by a mantle plume (Saunders et al., 1997), influencing the configuration of the plate boundary and increasing the volumes of eruptive products. The crustal thickness is still a matter of debate in Iceland (Palmason, 1980; Florenz and Gunnarsson, 1991) and is likely to be 20–35 km (Smallwood et al., 1999). A part of deformation in Iceland is distributed within the rift zone with its en échelon volcanic systems (Fig. 1a) consisting of volcanoes, magmatic fissures, normal faults and dilational fractures. Magmatic fissure is defined here as a linear eruptive source, served by deep-rooted dike-like feeders. The term dilational fracture is used when the displacement is primarily by movement normal to failure surface, but normal fault when it is parallel to failure surface. Most volcanic systems in Iceland are 40–80 km long and 10–15 km wide, and emanate from a central volcano (Saemundsson, 1978; Einarsson, 1991).

2. Field method

The work is based on detailed field studies of two neighboring volcanic systems: Fremri-Namur and Dyngjufjöl (Fig. 1a), situated within the Northern Volcanic Zone of Iceland and characterized by similar lithologies. The dimensions and orientations of faults of Sveinar, Sveinagja and Veggir graben (Fig. 1b) and the dilational fractures in these areas were measured in the field. The measurements here were made only along a part of each graben. However, all the data came from either the only areas available for structural analyses or from the most significant part of each graben. The lengths, throws and openings of the faults (Fig. 2a) were measured at intervals of 100 m along their lengths using a tape and a clinometer. We define the fracture length as the linear distance between the tips of a continuous surface rupture, and the fault opening as the maximum horizontal opening between the footwall and hanging wall of the fault measured normal to fault strike. Fault throw is measured as the maximum vertical displacement between the top of the footwall and the hanging wall, immediately beyond their tilted margins (Fig. 2a). This method avoids the complication of possible tilting along the edge of the hanging wall. The throw measured directly at the edge of the graben would result in its underestimation. Tilting of the hanging wall block of faults in Icelandic active rift zone is common and attributed to variations in subsidence, friction along the fault plane (Gudmundsson and Bäckström, 1991; Angelier et al., 1997) or monocline development due to upward fault propagation (Grant and Kattenhorn, 2004). Cumulative throw for stepped fault scarps is determined as the sum of the throws of all elements of the scarp. Throw gradient is defined here as the variation in throw per unit length of the fault.

The fault scarps of the Sveinar graben are covered by soil or grass locally, so the throw could only be constrained there with an accuracy of ± 3 m, but along the lengths of most faults throw was measured with an accuracy of ± 1 m. Faults of the Sveinar graben have significant dilational components. However, soil and grass obscured fault gaps at many locations, hence not allowing a reliable measurement of fault opening. The throw of faults along the Sveinagja graben could be determined (± 1 m) at all sites. However, there are some irregularities in opening along these faults that can be partly attributed to sand covering them locally. The interpretation involved in measuring portions of these faults with complex subsidence patterns may also contribute to an inaccuracy of ± 2 m in the estimation of the opening. The faults of the Veggir graben are well exposed, allowing measurement of the fault throw and opening to an accuracy of ± 1 m along most of their length. Locally, sand and tillite fill the fault openings along the western graben fault, resulting in errors in measured fault opening estimated at ± 3 m.

3. Geological setting

3.1. Fremri-Namur volcanic system

This volcanic system is located within the active rift zone of northeastern Iceland (Fig. 1a). The swarm of northerly-trending magmatic fissures is 160 km long and up to 17 km wide, and characterized by rhyolitic extrusions, large lava fields and basaltic flows (Fig. 1b). The central volcano domain (number 1 in Fig. 1b) is characterized by a high-temperature geothermal field. Voluminous fissure eruptions at Fremri-Namur have resulted in fields of recent lavas largely filling the innermost graben of the rift system. Subparallel magmatic fissures emanate from the center of the system and extend to the NNE and SSW. The three major magmatic fissures are: (i) Kraeduborgir which is 10 km long and is 2500–3000 years old; (ii) Raudholar-1, which is 6 km long and originated in the early Holocene; and (iii) Rauduborgir–Randarholar, which is 70 km long and is 6000–8000 years old. All these are expressed at the surface as crater rows.

Our detailed studies were carried out along the Sveinar graben, which lies along the central zone of the NNE-trending Rauduborgir–Randarholar crater row (Fig. 1b). The absence of glacial erosion or glacial infilling indicate that Sveinar faults post-dated the deglaciation (Thorarinsson, 1959). A large part of the Sveinar graben probably formed during the eruption of the Sveinar lava, 6000–8000 years ago (Gudmundsson and Bäckström, 1991). The graben was probably initiated by gradual prolongation of segments along strike as magmatic fissures opened up stepwise. The graben continued its formation in following rifting episodes, particularly propagating and deepening during the 1875 eruption. According to Thorarinsson (1959), the 1875 eruption began north of the Rauduborgir–Randarholar fissure and propagated SSW until it met the

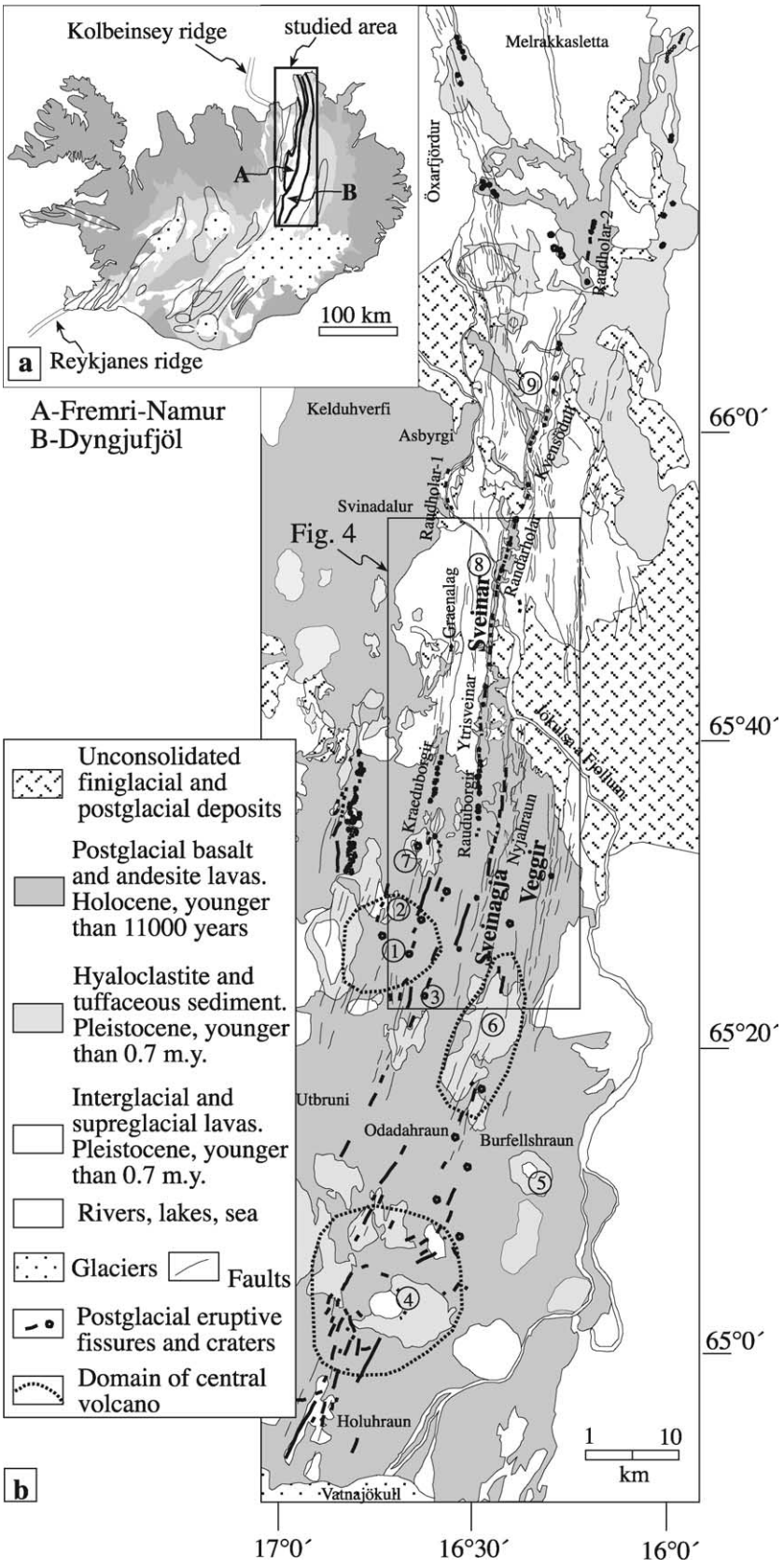

Fig. 1. Geological map of Fremri-Namur and Dyngjufjöl volcanic systems (a), adapted after Saemundsson (1977) and Johannesson and Saemundsson (1998). Encircled numbers: 1—Fremri-Namur volcanic center; 2—Ketildyngja lava shield; 3—Kerlingardyngja lava shield; 4—Askja volcanic center; 5—Herdubreid volcanic center; 6—Herdubreiddarfjöll; 7—Burfell; 8—Dettifoss waterfall; 9—Hafrafell. The inset map (b) shows the location of the studied volcanic systems: A—Fremri-Namur; B—Dyngjufjöl.

already existing graben; it then changed direction and followed the graben southward. Structural features found by Gudmundsson and Bäckström (1991) indicate that the course of the lava was locally directed by the existing portions of the graben and that displacement on graben faults continued after the eruption.

3.2. Dyngjufjöl volcanic system

This swarm of near-parallel magmatic fissures, 200 km long and up to 20 km wide, is located next to the volcanic system of Fremri-Namur (Fig. 1a). From its central volcano, Askja (number 4 in Fig. 1b), the system extends to the NNE to the northern coast of Iceland, and to the SSW at least as far as the Vatnajökull ice sheet (Fig. 1b). Sub-glacial volcanic activity resulted in the formation of hyaloclastite and pillow-lava ridges and post-glacial activity was mostly limited to the emplacement of basaltic magma (Sigurdsson and Sparks, 1978). A system of subparallel fissures emanates from the Askja volcano SSW where it encounters a glacier, obscuring possible evidence of fissure activity and NNE where it overlaps with the Herdubreid volcano (number 5 in Fig. 1b). The northern part of the fissure swarm is well expressed on the surface by crater rows, fractures and fault systems, including the Sveinagja and Veggir grabens.

The Sveinagja graben developed by several rifting episodes over thousands of years with at least some segments generated in Holocene times (Gudmundsson and Bäckström, 1991). The largest part of the present Sveinagja graben was probably formed before the voluminous extrusion of lava in 1875 (Sigurdsson and Sparks, 1978). Development of the graben continued in association with the 1872–1875 rifting episode, during which extension was accommodated by displacement on boundary faults and formation of new fractures (Gudmundsson and Bäckström, 1991). Most of the northern portion of the graben was covered by 1875 lava, while only limited outpourings of lava occurred to the south. As a result, the southern part of Sveinagja developed into the deep open graben observed at present. Some of the lava flow units flowed within an already existing graben, others have been faulted by a few meters subsequent to their emplacement (Sigurdsson and Sparks, 1978).

The formation of the Veggir graben remains somewhat obscure as, to our knowledge, there was no previous systematic study. The boundary faults of the Veggir dissect Holocene lava flows indicating that the graben, at least in its present form, developed in Holocene time. Similarly to the Sveinar and Sveinagja grabens, the faults of Veggir probably followed the growth of magmatic fissures and propagated stepwise northwards, away from Askja.

4. Structures of the Sveinar graben

4.1. Fracture distribution

The 0.5–0.8-km-wide Sveinar graben extends north–south for about 20 km (Fig. 2b). The area around it is characterized by a large number of normal faults (Fig. 2c and d) and dilational fractures that occur in clusters elongated subparallel to the main graben. Isolated normal faults are locally surrounded by short, subparallel dilational fractures that nucleated within 2–20 m of their tips. They also develop subparallel within 100 m of major faults (Fig. 3a), particularly where segments link (Fig. 3b and c). Such fractures are commonly absent within the next 700–800 m away from the graben faults, but beyond this distance they can again be observed. The strike of the 118 dilational fractures in the area shows a slight variation from south to north (Fig. 4). Most of these fractures in the southern sector strike N05°E$\pm$10° (Figs. 2b and 4, area 1). Here, linear arrays of isolated normal faults outside the graben are discontinuous and develop largely west of it. To the north, the strike of the dilational fractures is dominantly N350°W$\pm$10° and seems less irregular (Figs. 2b and 4, area 2). Clusters of these fractures are rather small and major normal faults are rare outside the graben. Most of the dilational fractures consist of subparallel linked segments (Fig. 5a). The widest openings are usually found in the middle part of each fracture segment. The lengths of 128 dilational fractures around the Sveinar graben vary from a few meters to 2–3 km (Fig. 5b). This length distribution appears to be best described by the least-square power-law function: $Y=5967X^{-1.0938}$. This function overpredicts the number of fractures shorter than 100 m, but the area possibly contains a large amount of short fractures, not sampled here.

4.2. Graben architecture

The boundary faults of Sveinar graben are discontinuous and consist of segments that have commonly 25–30 m offset (Fig. 2b). Major faults are subvertical at the surface (within $\sim$5° from vertical), with well-defined scarps (Fig. 2d). Fault segments are linear or slightly curved in a plane view and fault tips are distinct. Laboratory modeling shows that segmented fractures propagate and link in a different manner, depending on their initial spacing and overlap (Tentler, 2003a,b; Tentler and Temperley, 2003). Field observations in the Sveinar area allowed five major modes of fault segment interaction to be distinguished (Fig. 3c). Individual segments are either propagated toward each other by tips or they become linked by new intervening segments. Non-overlapping, closely-spaced fault segments (number 1 in Fig. 3c) tend to propagate along nearly straight paths toward each other. The tips of overlapping segments (number 2 in Fig. 3c) commonly propagate along curved paths that enclose an intervening core of intact material. The

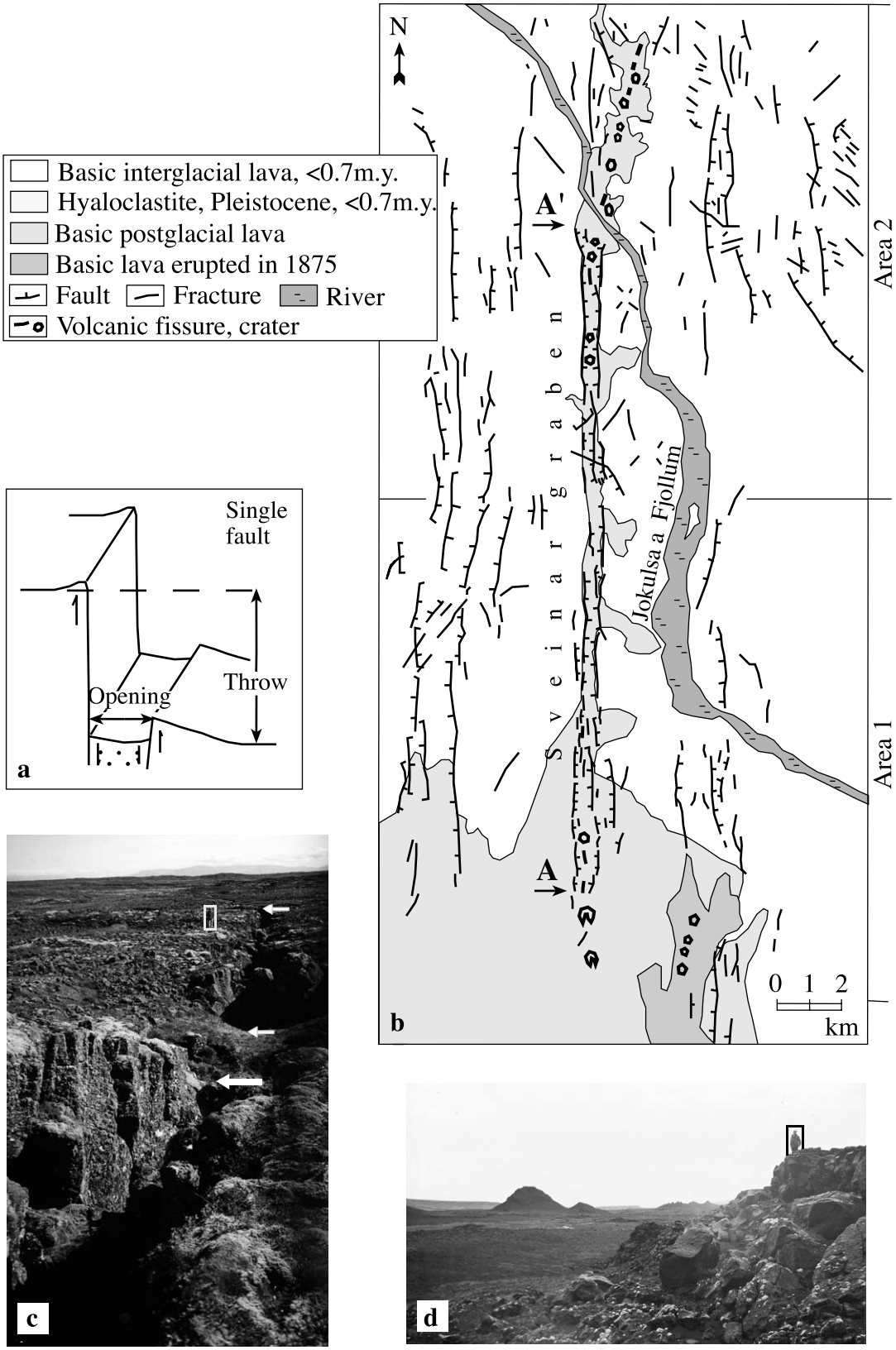

Fig. 2. Structure of the Sveinar graben. (a) Sketch showing the geometry, measured throw and opening of the graben faults. (b) Map of the graben area showing the studied sub-areas 1 and 2. Measurements were carried out along the line A–A′. (c) Normal fault, SW of the Sveinar graben, looking NE. The arrows show the tips of fault segments and the person indicates the scale. (d) The eastern boundary fault to Sveinar graben, looking NE, with the Rauduborgir–Randarholar crater row on the horizon. The framed person shows the scale.

curvature of tips in this case results from interaction of their stress fields (Pollard et al., 1982; Willemse, 1997; Maerten et al., 1999; Acocella et al., 2000; Walsh et al., 2003). In non-overlapping, widely-spaced fault segments (numbers 3 and 4 in Fig. 3c), usually only one tip propagates to the sidewall of the other. The tip of the other segment remains largely passive (number 3 in Fig. 3c) or propagates a short distance along its main strike (number 4 in Fig. 3c). Where non-overlapping fault segments are separated by a significant lateral distance (number 5 in Fig. 3c), they can link via an intervening segment(s). Such an intervening segment commonly develops from fractures nucleated in between tips of the major fault segments. Minor faults and fractures around the sites of fault segment linkage (Fig. 3b and c) apparently form as a result of partitioning of the regional extension associated with propagation of these segments towards linkage. Such minor fractures are commonly a few meters long, mostly either parallel to the main parts of the fault segments or to their curved tips.

The throws of faults bounding the Sveinar graben (Fig. 2b) were measured from A to A′ every 100 m along fault scarps (Fig. 2a). The average throw on both sides of the graben is 10 m with a maximum of 23 m (Fig. 6a). Maximum throws are offset from the center of both graben faults. On both fault scarps, the throw generally increases towards the north and deepens the graben. The distributions of throw along both fault scarps are generally similar, but the sites of throw amplification and reduction rarely match exactly across the graben. The variation of throw and tip zones distinguished along faults suggest that both faults were strongly segmented on a variety of scales. The length of the graben can be subdivided into four major segments (encircled numbers 1–4 in Fig. 6a) that, in turn, consist of smaller linked sub-segments (letters in Fig. 6a), all with boundaries marked by throw reduction. Most sub-segment boundaries match crudely across the graben (e.g. a, b, c of segment 3; b, c of segment 4). However, there are local anomalies of asymmetrical throw distribution on eastern

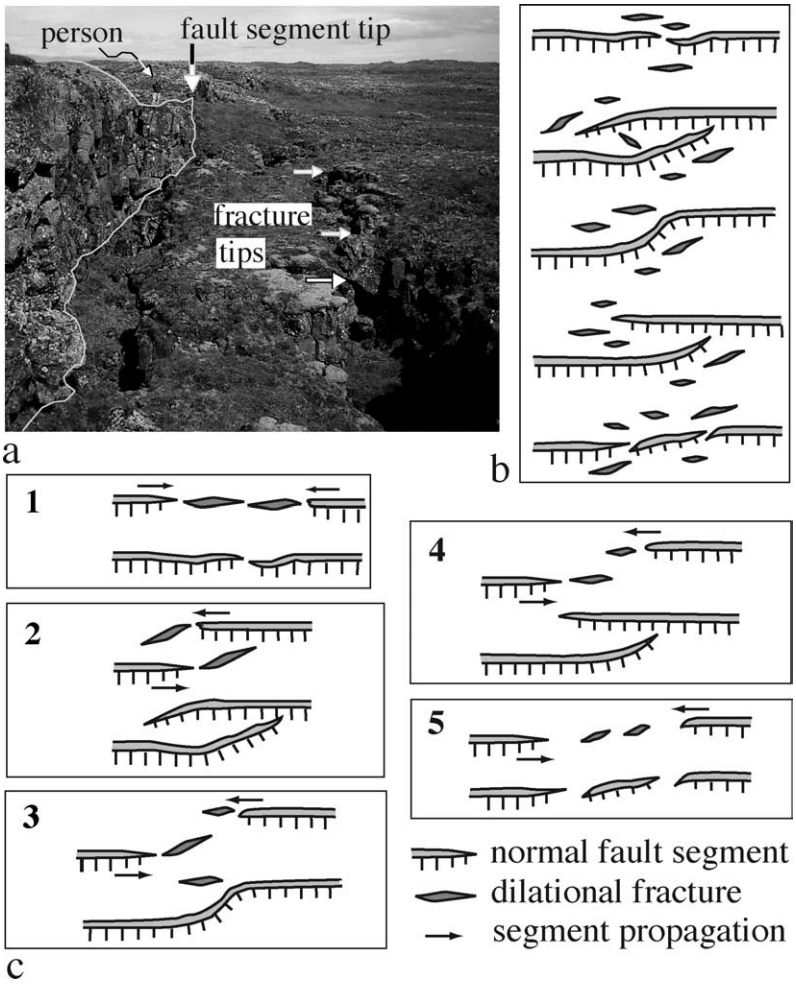

Fig. 3. Interaction of fault segments at the surface. (a) Northward view of a segment of the western boundary fault to Sveinar graben and subparallel dilational fractures. The arrows show the fracture tips and the person indicates the scale. (b) Distribution of the fractures in the zones of fault linkages. (c) Suggested modes of linkage of fault segments: 1—segments propagate along straight paths toward each other; 2—segments propagate to the sidewall of each other along curved paths; 3—one segment propagates to the sidewall of the other; 4—one segment propagates to the sidewall of the other, another segment propagates a short distance along its main strike; 5—segments link via an intervening segment(s).

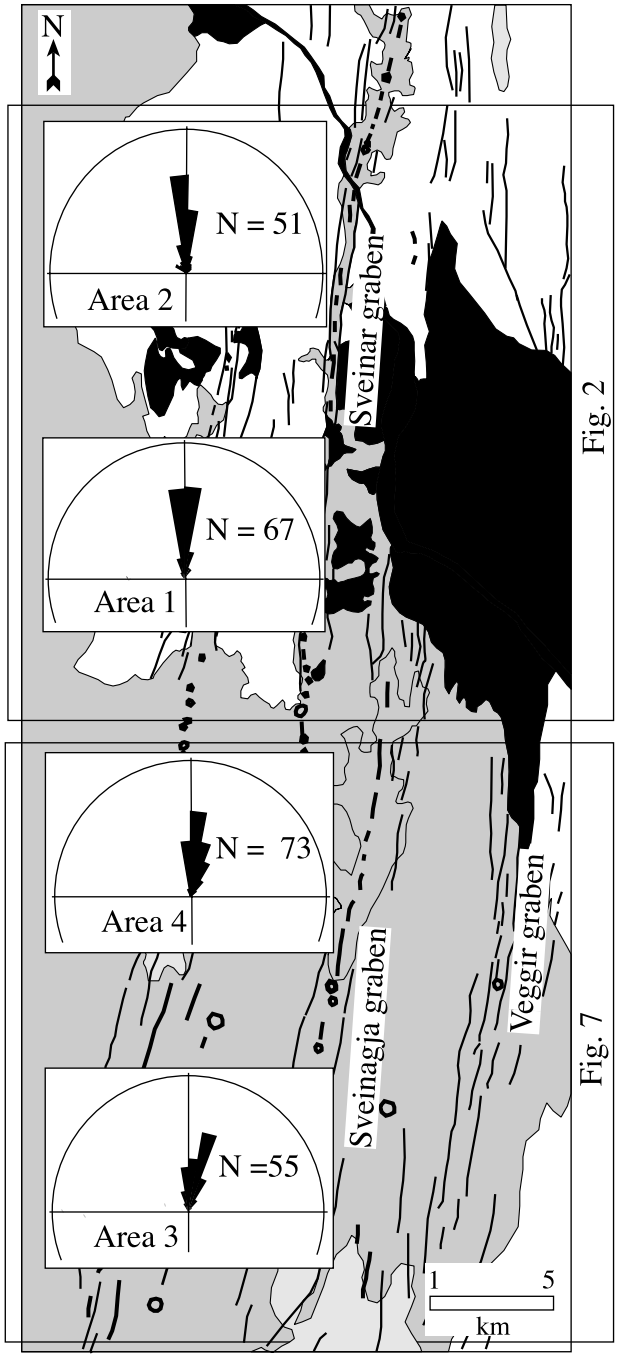

Fig. 4. Rose diagrams of strike distribution of dilational fractures sampled in four sub-areas around Sveinar, Sveinagja and Veggir grabens. Orientations of fractures change systematically from N10°–20°E in the south (area 3) to N350°–360°W in the north (area 2). Map adapted after Saemundsson (1977) and Johannesson and Saemundsson (1998) with changes.

and western faults. The sites of such anomalous throw reduction commonly correspond to segment or sub-segment boundaries. Thus throw is zero at 1.9–3.3 km along the eastern fault (at the tip of sub-segment a of segment 4), at 11.6–12.8 km along the western fault (at the tip of segment 3), and at 12.9–14.8 km along the eastern fault (at the tip of segment 2). The sites of asymmetrical throw amplification are common in the central parts of sub-segments, for example along c and d of segment 3. In the southern half of the graben, fault segments are shorter, with smaller throws and tips commonly obscured by the morphology of the lava flow. The northernmost segment 4 is the longest, with the highest throw and well-defined sub-segments. The local throw maximum of linked segments increases towards the center of the fault, although not always symmetrically. Both Sveinar faults exhibit asymmetric throw gradients that generally increase toward the segment tips and are independent of the segment length. Some segment interactions not marked by prominent throw reductions can still be recognized by an abrupt change in fault strike and somewhat smaller throw compared with neighboring parts of the fault.

The width of the graben ranges from 300 to 800 m (Fig. 6b). Variations in width only approximate its segmentation, so that fault segment tips do not generally correspond to the narrowest sites. Such width variation may probably partly be attributed to the complication of fault segments by curvature in a plane view. There is no clear correlation between graben width and fault throw so that the deepest and widest parts of the graben do not coincide.

5. Structures of the Sveinagja and Veggir grabens

5.1. Fracture distribution

The Sveinagja and Veggir grabens in the center of the Dyngjufjöll volcanic system (Fig. 1a), to the NNE of Askja and Herdubreiddarfjöll (number 6 in Fig. 1b) have similar strike and are surrounded by subparallel normal faults and dilational fractures, suggesting consistent stress patterns for the extensional domain (Fig. 7). Faults are discontinuous with segments some 30–50 m apart. Fractures have an irregular distribution; they are grouped in elongated clusters oriented parallel to the graben and develop mainly at their northern and southern continuation. Individual fractures are located within 50–100 m of the graben, around the tips of the faults and the segments, as in the Sveinar graben (Fig. 3c), but are rare within the next 500 m of each graben fault. Orientations of 128 dilational fractures change from N10°E–N20°E in the south (Figs. 4 and 7, area 3) to N0°–N10°E in the north (Figs. 4 and 7, area 4). The length–frequency distribution of fracture length can be approximated by the least-squares power function: $Y = 2704X^{-0.9683}$ with reasonably good data fit (Fig. 5c). Fractures in the area of the Sveinagja and Veggir grabens are only slightly longer than those around the Sveinar graben and their length distributions are similar.

5.2. Architecture of the Sveinagja graben

The graben is about 30 km long, 1–2 km wide and strikes N08°E (Fig. 7). Its eastern fault dissects postglacial

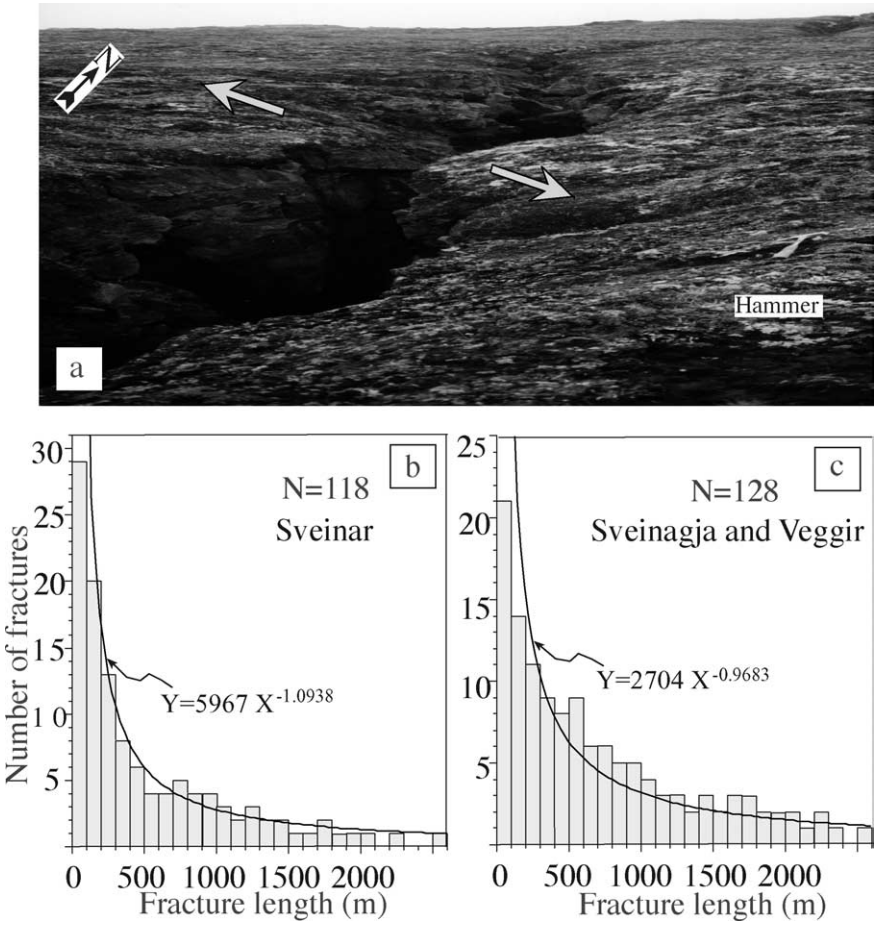

Fig. 5. (a) Tension fractures in basaltic lava of the Fremri-Namur volcanic system. The direction of extension is shown by arrows, the hammer gives the scale. (b) Histogram showing the length distribution of fractures around Sveinar graben. (c) Fracture length histogram for the Sveinagja and Veggir grabens.

pahoehoe lava along most of its length, while the western fault also dissects some younger aa lava from the volcano Ketildyngja (Gudmundsson and Bäckström, 1991). The graben consists of north and south parts that differ in the degree of fault exposure.

Prior to the 1875 eruption, the northern part of the graben was probably 10–15 km long, 400–500 m wide with throws of 10–20 m on its faults (Gudmundsson and Bäckström, 1991). At present the northern part of Sveinagja is 15 km long and is defined by faults with 4–10 m throw, largely filled with the Nyjahraun lava covering about 30 km^2 with an estimated volume of 0.3 km^3 erupted from the Sveinagja crater row (Gudmundsson and Bäckström, 1991). The magmatic fissure is flanked by a row of spatter cones and consists of irregular segments of various lengths that are offset by 30–40 m (Sigurdsson and Sparks, 1978). The poorly defined faults of the northern part of Sveinagja have not reactivated since the 1875 eruption (Gudmundsson and Bäckström, 1991). Extensional structures developed in this part of Sveinagja cover a wide area and the graben structure is not well defined. The 1875s Nyjahraun lava crops out only in small isolated patches in the southern part of the Sveinagja graben, that is 9 km long, 1–1.7 km wide, and it strikes N07°E. Post-1875 activity has increased the throw of the graben faults (Gudmundsson and Bäckström, 1991), making the fault scarp of the southern segment prominent, symmetrical about the magmatic fissure, particularly so at its northern part. The faults at the southernmost end of this segment have less regular spacing and orientations.

Because the northern part of Sveinagja is largely obscured by lava, our field study focused on its southern segment with well-exposed and continuous faults. These consist of segments with dilational fractures being common around sites of their linkage, similarly to structures of the Sveinar graben (Fig. 3b). Five modes of segment interaction defined along the Sveinar graben (Fig. 3c) are also distinguished along Sveinagja. Measurements were carried out in the southern part of the graben at an interval of 100 m along the line B–B′ (Fig. 7).

Faults of the Sveinagja graben are subvertical, with openings at the surface and are commonly complicated by fault-bounded relay ramps collapsed into the open fault zone (Fig. 8a). The maximum throws, up to 17 m, occur near the center of each fault and they taper off toward the tips (Fig. 9a). Although variation in fault throw is largely similar on both sides of Sveinagja, sites of local throw amplification

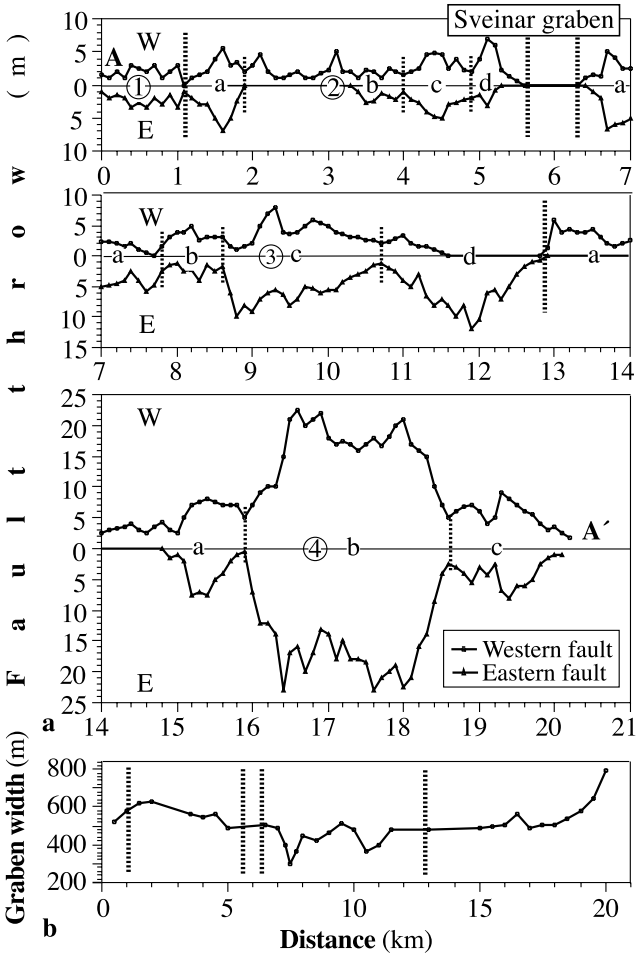

Fig. 6. (a) Throw profiles for the western (black circles) and eastern (black triangles) boundary faults along the line A–A′ (Fig. 2b) of Sveinar graben. (b) Graben width profile along the line A–A′ of the Sveinar graben. Encircled numbers 1–4 indicate segments, letters a–d indicate sub-segments, dotted lines show segment and sub-segment boundaries.

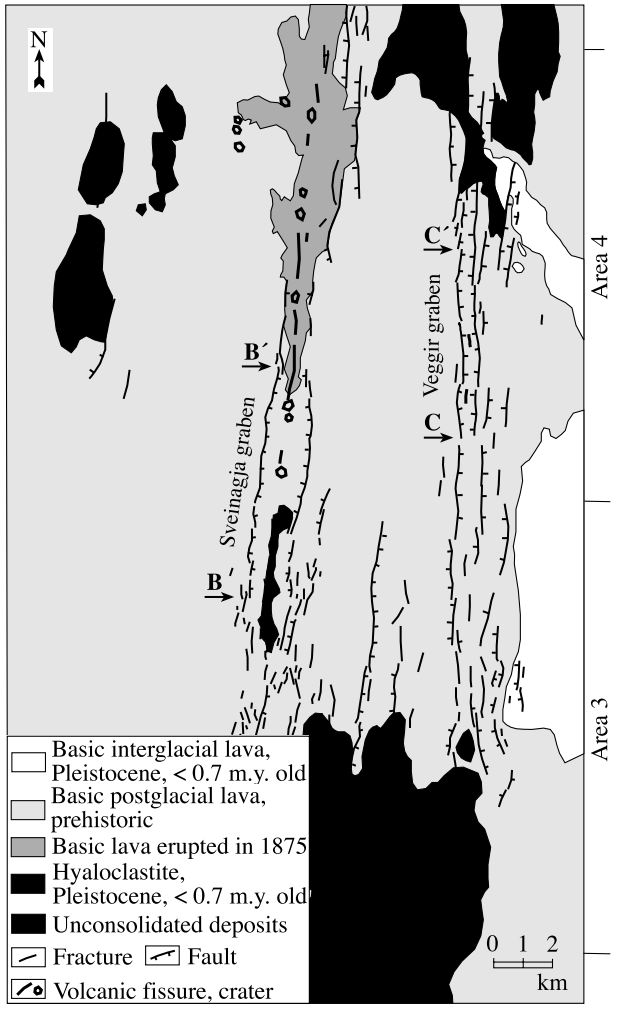

Fig. 7. Map of Sveinagja and Veggir grabens showing the sampling areas 3 and 4. Measurements were carried out along the lines B–B′ and C–C′. Map adapted after Saemundsson (1977) and Johannesson and Saemundsson (1998) with changes.

match only locally across the graben. Four major linked segments with boundaries, distinguished by throw reduction and geometries of their tip zones, are numbered in Fig. 9a. Segments increase in length and throw northward. Local anomalies of asymmetrical throw distribution on faults across the graben are mainly throw reductions related to segment boundaries, such as at 2.8–3 km along the western fault near the tip of segment 3 and at 6.8–7.3 km along the eastern fault between segments 3 and 4. Throw gradients are significant near segment tips and highest for segment 3.

Fault opening varies along the faults (Fig. 9b), and the maximum opening is in the southern part of both faults (13 m on the western fault and 11 m on the eastern fault). The shape of the curve for each fault departs from elliptical, particularly so for the eastern fault. Boundaries of all segments defined by reduction in throw (Fig. 9a) are also distinguished by reduction in opening (Fig. 9b). Variation in opening along the faults is significantly larger compared with variation in throw, particularly along segment 3 where the throw is large. Local anomalies of asymmetrical opening distribution on faults across the graben also occur mainly along segment 3, at 3.9–4.1, 4.5, and 4.8–5.1 km.

The width of the Sveinagja graben ranges between a maximum of 1630 m and a minimum of 1030 m along the line B–B′ (Fig. 9c). The graben is generally wider at its central part and widest along the longest segment 3 at 4.3–5.2 and 5.8–6.2 km. It narrows gently towards its northern end at about 7300 m and at three intervening points along it: at 1, 2.3, and 3.8 km. The width fluctuates depending on the segment location and degree of symmetry across the graben. Width reductions roughly correspond to the boundaries of the graben segments except for the width minimum at 3.8 km along segment 3. Fluctuations in graben width are also imposed by the shape of the fault segments in plane view, particularly their commonly enhanced curvature at tips. Although the sites of highest fault throw and opening

along the graben do not coincide with its widest parts, the pattern of graben segmentation may be distinguished by correlation of locations of reductions in fault throw and opening with graben width (Fig. 9).

5.3. Architecture of the Veggir graben

The Veggir graben is 12 km long, 400–600 m wide and oriented N02°E (Fig. 7). The graben consists of segments at different stages of linkage, achieved mainly by curving propagating tips (modes 2–4 in Fig. 3c). The discontinuous graben faults are curved in plane view in the southern part of Veggir and straighter to the north. Faults are vertical at the surface, with prominent, sharp scarps (Fig. 8b). Their segmentation is well-expressed, with sites of segment linkage marked by a throw reduction and curvature of interacting tips and abundant dilational fractures around, similarly to segments of the Sveinar graben (Fig. 3). Minor fractures beside the fault surfaces often form damage zones with collapsed portions of fault scarps. Measurements were carried out every 100 m along the graben along the line C–C′ (Fig. 7).

The average throw of the Veggir graben is 10 m, while the maximum throw reaches 18 m on the western fault and 20 m on the eastern fault (Fig. 10a), slightly exceeding those for the Sveinagja graben. In general, variations in throw along both faults are similar with points of relative throw reduction roughly corresponding on both sides of the graben. The highest throws are within the central portion of the graben (segment 2) with a shift of some 400 m between the western and eastern faults. The throw distribution on both faults is largely symmetrical along the graben with respect to the center of the fault length and roughly close to elliptical. Four major graben segments can be further subdivided into shorter, linked sub-segments (Fig. 10a). The variability in the throw profile is highest for segment 2, which is also the longest and approximately central. Some sites of segment linkage do not have characteristic throw reductions, as for faults of the Sveinar graben. Throw gradients increase near segment tips and are higher for longer segments with correspondingly larger throws.

The fault opening is significant on both faults of the Veggir graben (Fig. 10b), while it is largest along segments 2 and 3. The average opening is 4 m for the western fault and 3 m for the eastern fault, while the maximum opening is 10 m for the western fault and 9 m for the eastern fault. Although the two graben faults show generally similar

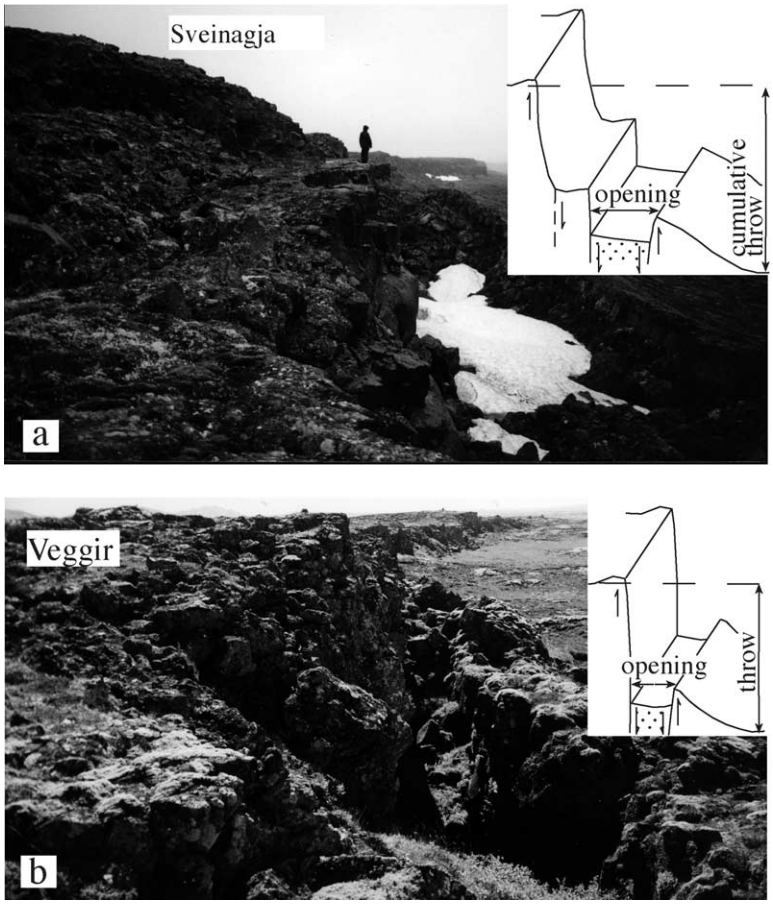

Fig. 8. Structure of the single fault of Sveinagja graben (a) looking north and Veggir graben (b) looking NNW, and the sketches of their geometry and measured parameters.

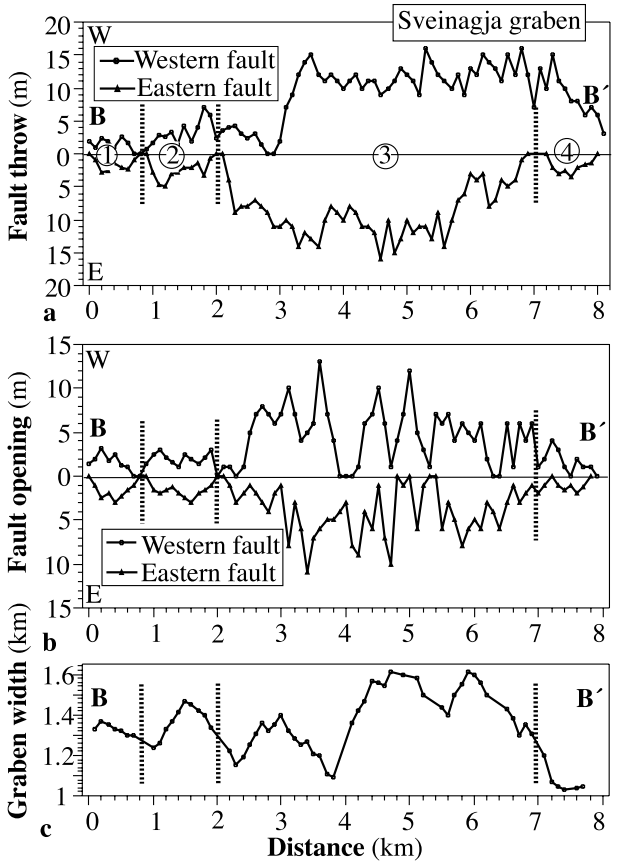

Fig. 9. Measurements along the line B–B′ (Fig. 7) of Sveinagja graben. Fault throw (a), fault opening (b), and width of the graben (c). Values for the western faults are shown by black circles and for the eastern fault by black triangles. Encircled numbers 1–4 indicate segments, dotted lines show segment boundaries.

variation in dilation, particularly in location of opening reduction, there are local anomalies of asymmetrical maximum opening on faults across the graben. These are particularly significant along segment 2, where the largest opening along the western fault is at 2.7–3.9 km, but along the eastern fault at 3.2 and 4.3 km. As in the case of the Sveinagja graben (Fig. 9), there is no good correlation between fault throw (Fig. 10a) and opening (Fig. 10b) with a significant shift of 400–500 m between the maximum throw and maximum opening of both faults. However, four segments along each fault of the graben on throw profiles can also be identified on the grounds of variation in the opening.

The graben width for most of the length of Veggir is 500–600 m with variations at least partly related to its segmentation (Fig. 10c). Thus, it widens to 580–630 m in the central parts of segments 1 (at 1–1.6 km) and 2 (2.7–3.3 km) and to 640 m at the boundary between segments 3 and 4 (at 4.7–5.3 km). The graben is narrowest at its southern end, reaching 430 m, and narrows gently to 470 m between segments 1 and 2, and 2 and 3, as well as at its northern end. The tendency towards graben narrowing at sites of segment linkage probably results from the fault interaction pattern. At the sites of coalescence, segment tips commonly propagate along curved inward, towards the graben axis, before linking (Figs. 3a(2–4) and 7), resulting in the narrowing of the graben, as may have occurred for interaction of segments 1+2 and 2+3. The geometry of interaction is different between segments 3 and 4, where segment 4 of the eastern fault trends slightly oblique to segment 3 and curves outwards, away from the graben axis before linking with segment 3, resulting in a local widening of the graben.

6. Discussion

6.1. Fracture orientation, distribution and length

Variations in fracture strike in our study suggests a direction of maximum extension changing from about N110° in the south of the study area to about N80° in the north. There are at least three contributing factors that might account for this swing in trend. First, the orientation of the axial rift zone of Iceland changes from N15°E in the vicinity of Vatnajökull glacier to N00E approaching the northern

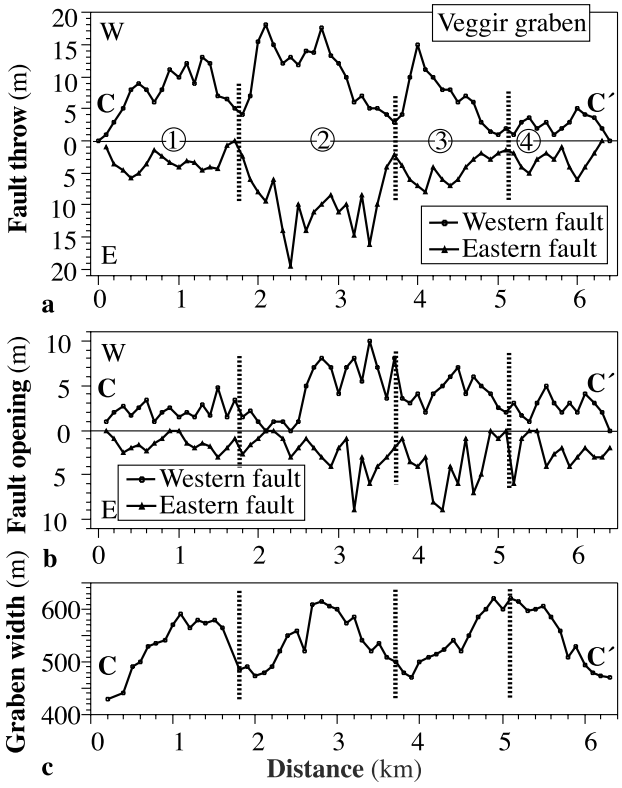

Fig. 10. Measurements along the line C–C′ (Fig. 7) of Veggir graben. Fault throw (a), fault opening (b), and width of the graben (c). Values for the western faults are shown by black circles and for the eastern fault by black triangles. Encircled numbers 1–4 indicate segments, dotted lines show segment boundaries.

coast (Bergerat et al., 1990). Second, interaction takes place between the spreading axis on Iceland's northern coast and the transform faults in the Tjörnes fracture zone. Fissure swarms near the northern coast do not quite strike parallel to the rift zone axis (Sigurdsson and Sparks, 1978; Rögnvaldsson et al., 1998), which may account for the strike of fractures in this study. Third, fracture orientations probably reflect the general curvature of fissures emanating from the central volcano (Gudmundsson, 2000).

Dilational fractures form within 50–100 m of the graben faults, particularly where segments interact. Most of them develop as process zone fractures as fault segments propagate laterally. Few of the isolated faults and fractures occur within the next 500–800 m of the graben faults, although this distance varies between grabens and depends on the length of the corresponding fault segment. Such fracture distribution indicates stress shadows flanking grabens as stresses cannot be transmitted across the free surface of a fault (Ackermann and Schlische, 1997; Willemse, 1997). Most isolated normal faults here have the single semi-continuous scarps with aligned segments, common for small faults in Iceland (Gudmundsson, 1987a; Angelier et al., 1997). By contrast, graben faults consist of closely spaced overlapping segments with their interaction resulting in composite structure with a collapsed block of rock between fault walls, common along large faults in Iceland (Acocella et al., 2000; Grant and Kattenhorn, 2004).

The fracture length distribution (Fig. 5) shows that relatively short fractures are more common than the long ones, as occurs elsewhere along the rift zone of Iceland (Gudmundsson, 1987a,b, 2000). Fracture size distribution can be characterized as power-law, albeit with an exponent that varies for different fault populations (Cowie and Scholz, 1992; Watterson et al., 1996). Power-law and exponential populations probably develop in different strain regimes when fractures reach a certain density (Gupta and Scholz, 2000). Most fracture populations in oceanic crust are described by exponential functions (Carbotte and Macdonald, 1994; Cowie et al., 1994). However, the distribution of fracture length in this study best fits power-law functions (Fig. 5b and c), as common for fractures in continental crust (Watterson et al., 1996; Cowie, 1998). Icelandic crust is influenced by a mantle plume resulting in its thickness (20–35 km) being more similar to that of typical continental rather than oceanic crust. Such thickened crust might be the reason for fracture populations developing in a strain regime common on continents, with the resulting power-law fracture length distribution obtained in this study and reported by Gudmundsson (1987a,b) for fractures in southwest Iceland.

6.2. Fault throw and propagation

Elastic fracture mechanics theory predicts that the throw on an ideal fault surface is elliptical and decreases from a central maximum to zero at the tip-line (Walsh and Watterson, 1987). The throw profiles in Figs. 6a, 9a and 10a follow an elliptical pattern, as was interpreted by Gudmundsson and Bäckström (1991) for the Sveinagja graben, but only in the very broadest sense, when exclusively throw maximums of segments along a fault are compared. In detail, profiles largely depart from self-similar elliptical shape with throw varying non-systematically and larger than predicted by models for the propagation of a fault surface in a homogeneous elastic medium (Walsh and Watterson, 1987; Cowie and Scholz, 1992; Watterson et al., 1996). Such oscillating profiles are expected if the present throw accumulated by successive increments (Dawers et al., 1993). Recent field studies (Wilkins and Gross, 2002; Gawthorpe et al., 2003; Mazzoli and Di Bucci, 2003) and theoretical models (Maerten et al., 1999; Walsh et al., 2002, 2003) also advocate such complex throw distribution. Profiles analyzed here thus represent combined patterns of throw distribution on the fault segments, which occurred in a succession of rupture events as the fault planes grew. Throw gradients along our faults are highest near segment tips as predicted by linear elastic fracture mechanics models (Cowie and Scholz, 1992; Watterson et al., 1996; Willemse, 1997; Walsh et al., 2003) where a throw reduction at the tip determines the finite stress concentration (Dawers et al., 1993). The observed variation in throw gradients at segment tips indicates that a concentration of stress there is not simply a measure of rock strength, but depends also on the location of segments and their mutual orientation (Cartwright et al., 1995; Cowie, 1998; Acocella et al., 2000). High throw gradients of some of the near tip segments may also reflect a slight reactivation of portion(s) of graben.

Profiles of graben faults here reveal a few orders of segmentation allowing a speculative reconstruction of the history of segment linkage (Fig. 11). We assume that the growth rate is the same for each segment within the considered fault (i.e. the amount of throw of each segment is a measure of its stage of evolution). Thus the location of maximum throw on a fault represents where it nucleated (Dawers and Anders, 1995; Kattenhorn and Pollard, 2001) and location of throw reduction indicates site of segment linkage (Walsh et al., 2003).

The linked segments of faults (Figs. 6a, 9a and 10a) suggest their incremental growth (Fig. 11a and b) where large segments resulting from the coalescence of several smaller sub-segments typically show several asymmetric maximum throws (Fig. 11c). Throw variations are relatively symmetrical with respect to the maximum throw for the Sveinagja and Veggir grabens (Figs. 9a and 10a). However, the southernmost part of the Sveinagja fault (Fig. 9a) and the northernmost part of the Veggir fault (Fig. 10a), are both characterized by short, linked segments with low throw contrasting the abrupt throw decrease at the opposite ends of faults. Such asymmetrical throw distribution at the opposite ends of faults have been attributed to differences in segment length, slip rates, or mechanical interaction effects (Cowie

and Scholz, 1992; Cartwright et al., 1995; Wilkins and Gross, 2002). Alternatively, such throw distribution may indicate different rates of lateral propagation from the center of the fault towards each of the fault tips (Fig. 11a and b). In this way, rapidly and continuously propagated fault tips would be recognized by an abrupt decrease of throw, whereas slowly and episodically propagated fault tips would be marked by short sub-segments with consistently low throw. Another possibility is that the maximum throw on each fault is where the fault could preferentially be reactivated over time by slip events. Such a mechanism could have been the case for the Sveinar faults that have highly asymmetric throw profiles decreasing from a maximum at the northern end towards lower values in the south (Fig. 6a). Such patterns were attributed to mechanical interaction between segments (Willemse, 1997; Maerten et al., 1999), but can be alternatively explained by strongly south-directed graben propagation. Our data (Figs. 6a and 9a) confirm that throw profiles increasingly differ from the theoretical profiles as faults increase in length (Walsh and Watterson, 1987). This difference is due to larger effects of segment interaction and/or asymmetry of lateral fault propagation.

Throw profiles of longer segments usually reflect coalescence of their sub-segments. Recent coalescence of two sub-segments results in a throw deficit with respect to the new, increased length of the segment (Fig. 11c (i)). This stage is commonly followed by a period of throw re-equilibration for a lengthened segment to compensate its throw deficit and satisfy the displacement–length scaling (Cowie, 1998). Post-linkage strain accommodation results in retardation of lateral propagation and accumulation of throw at the site of linkage (Fig. 11c (ii)). This stage of throw accumulation can be also recognized on the throw profile by the higher throw gradient at segments tips. Throw compensation lasts until the critical fault displacement profile is re-established (Cartwright et al., 1995) and tip propagation then resumes (Fig. 11c (iii)). Separate segment tips often link by an intermediate segment with lower throw (Fig. 11c (iii)). When segments nucleate simultaneously equal distances apart (Fig. 11d (i)), they commonly propagate laterally (Fig. 11d (ii)) while throw accumulation is retarded until their tips link (Fig. 11d (iii)), as was also described by Kattenhorn and Pollard (2001). In this way, sub-segments that have linked at early stages of extension can often be recognized by high values and gradients of throw while those that coalesced later are under-displaced (Fig. 11e).

The plot of length of linked segments along a fault against the maximum throw for the three grabens (Fig. 12a) shows that throw increases with length. A large scatter, also reported in other data sets, was interpreted as caused by the methods of data collection or local variations in rock properties (Walsh and Watterson, 1987; Cowie and Scholz, 1992). However, in our case, we infer that most of the scatter resulted from the complexity of the fault surfaces as they grew. Throw is expected to be more evenly distributed than documented here if segments have linked into continuous faults at the early stage of graben development and slip took place along the entire fault lengths (Willemse, 1997; Cowie, 1998). Large variation in throw suggests that faults experienced multiple slip events where slip was not continuous, but rather occurred in local increments resulting in at least three orders of segmentation. The migration of the locus of preferred throw accumulation (Fig. 11) can lead to anomalies in throw distribution, local asymmetry in throw across the graben (Figs. 6a, 9a and 10a) and deviations from the mean length/throw ratio (Fig. 12a). Slip of individual segments at the same time as they propagated laterally would account for throw being proportional to segment length (Walsh and Watterson, 1987; Dawers and Anders, 1995; Maerten et al., 1999), whereas large scatter (Fig. 12a) suggests that faults are likely to grow in intervening stages of lateral propagation and throw accumulation. The plot of fault length versus maximum throw for isolated faults shows a markedly smaller scatter around the length/throw mean value and is consistent with linear scaling (Fig. 12a). Fault displacement in rock with uniform mechanical properties is given by $d = \gamma L$, where the parameter γ depends mainly on the ratio of the shear strength to elastic rigidity of the faulted rock. Fault populations in the same tectonic settings and rock types are predicted to exhibit similar d/L ratios (Cowie and Scholz, 1992; Cowie, 1998). For the faults analyzed here, the mean throw–length ratio is 0.006 (Fig. 12a). Deviations above and below this value reflect the different distances over which each fault propagated laterally and are likely to be a function of the rate of tip propagation, mechanical segment interaction and differences in fault overlap to fault spacing. The linear relationship between fault length and throw observed here ($d/L < 0.01$) lies within the range of those documented along the Mid-Atlantic Ridge (Bohnestiehl and Kleinrock, 2000), East Pacific Rise (Carbotte and Macdonald, 1994; Cowie et al., 1994) and in northeast Iceland (Opheim and Gudmundsson, 1989).

6.3. Fault opening

Normal faults in this study have a dilational component (Figs. 8, 9b and 10b) for most of their lengths, as is common for faults throughout the rift zone of Iceland (Acocella et al., 2000; Gudmundsson, 2000; Grant and Kattenhorn, 2004). Their opening is variable, but generally is greatest near the middle of the fault (Gudmundsson, 1987b). Shorter segments tend to have smaller openings (Fig. 12b), although the scatter in the data is large. There are no simple length/opening and throw/opening relationships along normal faults in Iceland (Gudmundsson, 1987a). A possible explanation for this could be that length and throw of fault segments are not dominant factors controlling their opening. The correlation between segment opening and throw for the Sveinagja and Veggir faults (Fig. 12d–g) appears to be

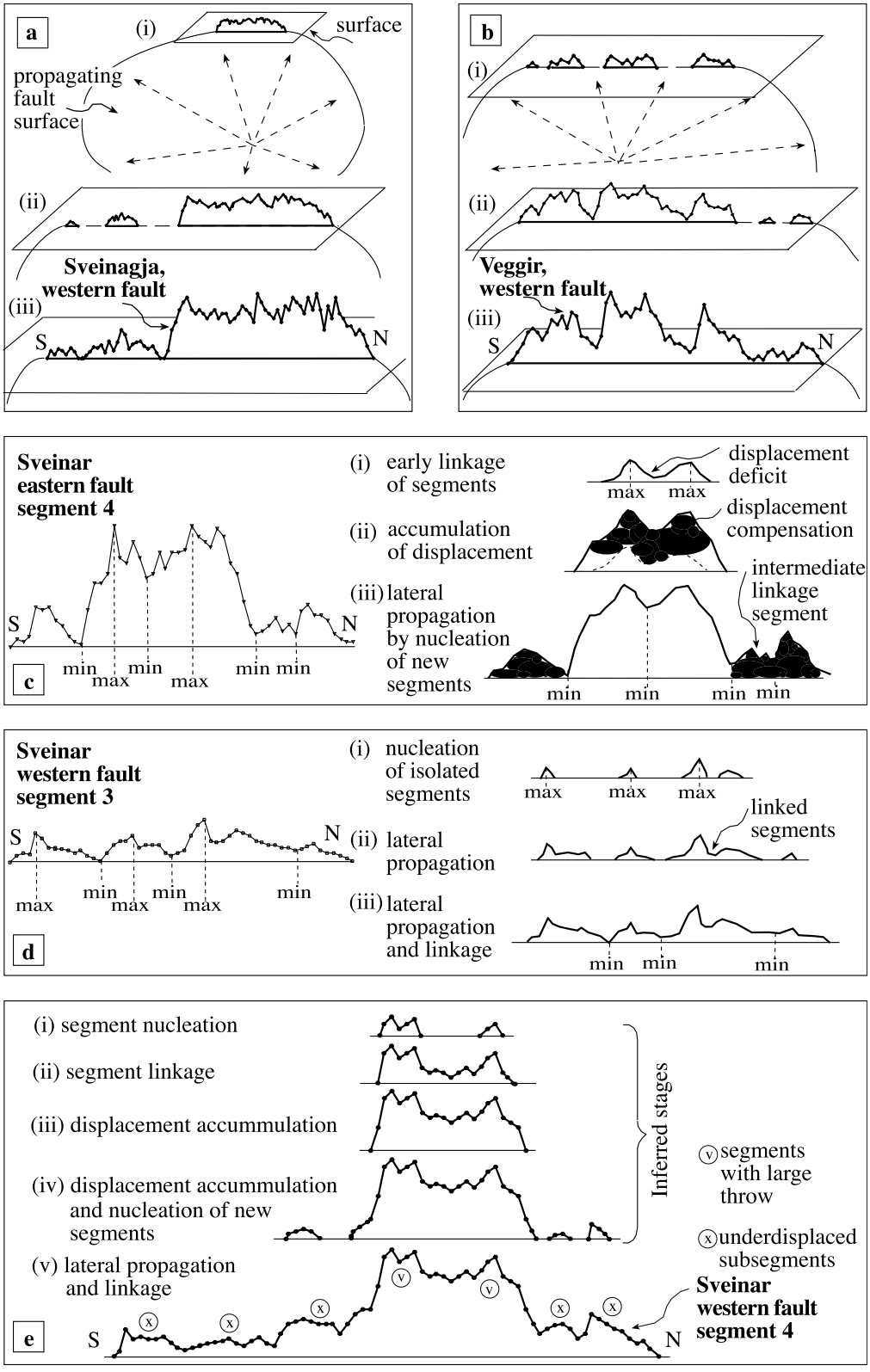

Fig. 11. Diagrams speculating how the upward propagation of the fault plane accounts for the throw pattern of the western faults of: (a) Sveinagja and (b) Veggir grabens. The fault does not reach the surface in the regions where throw is zero between segments; (i)–(iii) are stages of fault propagation. (c) Stages of growth for segment 4 of the eastern fault; (d) segment 3 of the western fault; (e) segment 4 of the western fault of Sveinar graben.

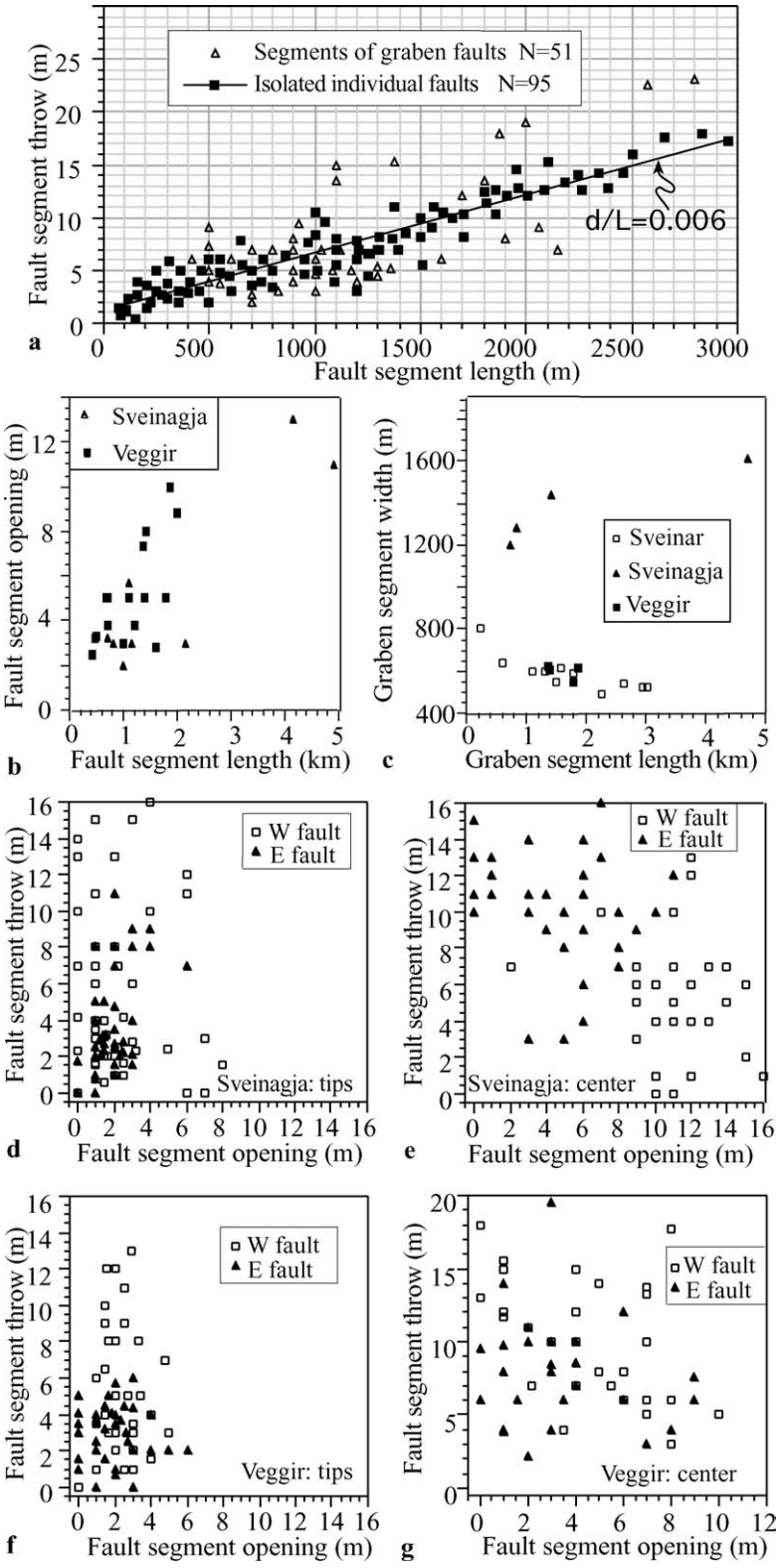

Fig. 12. Diagram correlating parameters of normal faults. (a) Fault length versus maximum throw for segments of graben faults (open triangles), and for isolated individual faults (black squares) within and around the three graben. The straight line $d/L = 0.006$ is fitted through data indicating a linear relationship between fault length and throw. Deviations above and below this value reflect the different distances over which each fault propagated laterally. (b) Fault segment length versus maximum opening along segments of Sveinagja and Veggir grabens. (c) Graben segment length versus maximum width of the three grabens. (d) Segment opening versus throw near the fault tips, and (e) near the fault centers of Sveinagja faults. (f) The same for the segments of Veggir near the fault tips, and (g) near the fault centers.

generally weak, but has significantly different patterns for segments at fault tips (Fig. 12d and f) compared with segments near fault centers (Fig. 12e and g). Segment opening/throw for the fault tips (Fig. 12d and f) shows a significant clustering of data, whereas that for the fault centers shows a larger scatter (Fig. 12e and g). Such a difference in clustering for fault tips and middles may be related to distinct stages in growth of corresponding fault segments. Segments at propagating fault tips are commonly at the early stages of displacement, with a small throw and opening. Segments in the central parts of faults have undergone a longer history of growth; they are in a more mature stage of interaction where throw and opening of each sub-segment results from a larger number of displacement episodes and thus may show a higher scatter. Data points for central parts of eastern and western faults of Sveinagja are grouped into overlapping but distinctive areas (Fig. 12e). Such a pattern could result from the variation in the increments of fault growth across a wide graben. On the contrary, data points for faults of the Veggir graben, which is about three times narrower, are not grouped for each fault (Fig. 12g), indicating more similarity in fault formation across it.

The opening observed along faults in this study is significant and comparable with their throw. The total dilation needed for the formation the graben faults is likely to be even greater, as it commonly exceeds fault opening measured in situ (Gudmundsson, 1987b), while Fremri-Namur and Dyngjufjöl volcanic systems represent only a fraction of the total dilation across the spreading zone. Although the opening along analyzed faults may be considered as local (as manifested only by faults within the active rift zone) and superficial (as present only in shallow, exposed portions of faults), it characterizes the important stage of fault formation on the surface, where most geological data is collected. The documented opening also emphasizes the significance of the dilational component that may be present along the entire fault plane but obscured at depth where it may be accommodated by other mechanisms, such as diking.

The dilation characteristic of normal faults in the rift zone of Iceland has been also documented along continental normal faults (Muffler et al., 1994). Similar features occur on the flanks of shield volcanoes on ocean islands, such as Hawaii (Peacock and Parfitt, 2002). However, to our knowledge, such an opening has not been reported for faults on the ocean floor. Nevertheless, the development of normal faults along submarine ridges is controlled by tectono-magmatic conditions similar to those operating in Iceland. It is possible that oceanic faults also initiate with an opening that is not easy to be preserved and recognized in the marine environment. Such faults are partially buried by basaltic flows and unconsolidated sediments at the base of their scarps along the axes of both fast- (Macdonald et al., 1996; Carbotte et al., 1997) and slow-spreading ridges (Tucholke and Lin, 1994; Karson, 1998). However, even if openings along oceanic faults are unlikely to survive in a great number beneath the weight of water column and sediments, the possibility of their existence during fault formation should not be ruled out. The presence of dilational components along normal faults is of general importance for understanding their mechanics and is an obvious topic for future research.

6.4. Graben width

The width of graben segments does not appear to be simply proportional to their length (Fig. 12c). Thus for a wide graben like Sveinagja, segment width increases with length, while for a narrow graben such as Sveinar and Veggir, segments are narrower with increasing length. This apparent absence of simple length/width correlation may be attributed to a difference in fault depth profiles and segment interaction (Cartwright et al., 1995; Angelier et al., 1997). Alternatively, it may be related to variations in dynamics of magma beneath the graben. Within the rift zone of Iceland, two main mechanisms have been suggested for the transport of magma to the site of eruption. The first implies lateral movement of magma along a propagating fissure, at portions of volcanic systems located relatively close to the crustal magma chamber beneath the central volcano (Sigurdsson and Sparks, 1978; Einarsson, 1991). The second mechanism involves dykes formed by magma ascending vertically from a deep-seated magma reservoir that occurs at larger lateral distances from the central volcano (Thayer et al., 1981; Gudmundsson, 2000). In any case, magma propagating laterally and/or vertically along fissures at depths of 2–7 km may lead to the subsidence at the surface initiating formation of a graben (Rubin and Pollard, 1988; Einarsson, 1991). Correspondingly, fault initiation, segmentation and, possibly, displacement in a graben would be dependent not only upon the stress field and mechanical properties of faulted rocks, but also on the parameters related to magma dynamics. The depth of the propagating magmatic fissure, the rate of its propagation, and the volume of magma may vary between different grabens resulting in varied length/width relationships of graben segments.

6.5. Graben study in Iceland

Numerous sea-floor observations in recent decades have documented surface normal faulting throughout the axial depressions and on the flanks of mid-ocean ridges where steep (70–90°) fault scarps commonly have throws of a few tens of meters (Carbotte and Macdonald, 1994; Tucholke and Lin, 1994; Cowie, 1998; Macdonald, 1998). Faults often form graben systems, shallow and short in the early stages of the extensional cycle, but progressively deepening, lengthening, and becoming more asymmetric as extension continues (Macdonald et al., 1996; Carbotte et al., 1997). Direct access to structures in Iceland, allowing field

measurements, raises the possibility for a more thorough understanding of fault geometry and kinematics than submarine data sampling. The results of the present study should be applicable to structures on the ocean floor that are, despite the absence of mantle plume-related complications (Saunders et al., 1997), probably operated by similar mechanical processes (Angelier et al., 1997; Acocella et al., 2000; Gudmundsson, 2000; Grant and Kattenhorn, 2004). Fault growth occurs in stages of throw accumulation, opening and lateral propagation speculatively inferred in this study, which alternate and superimpose in space and time. Such stages may generally characterize development of normal faults at divergent plate boundaries.

7. Conclusions

1. Grabens bounded by discontinuous normal faults consisting of linked segments, analyzed in this study, are common structures of volcanic systems within the active rift zone of Iceland.
2. Graben, isolated normal faults and dilational fractures of the Fremri-Namur and Dyngjufjöl volcanic systems typically develop within elongated domains in areas of high extension. Dilational fractures are common near the sites of fault segment linkage but unusual beyond 500 m to 700–800 m of graben faults, suggesting a stress shadow zone surrounding graben.
3. The dimensions of individual fractures may be controlled by the fracture toughness of rocks, average propagation velocity, the distribution of pre-existing crustal weaknesses, geometry of already formed fractures and relaxation of tensile stress in their vicinity. Length–frequency distributions of fractures in the studied areas are best described by power-law functions. The anomalously thick crust in Iceland might account for such fracture length distribution otherwise more commonly found in continental crust.
4. The widths of the graben segments is not simply a function of their length or fault throw, which may be accounted for by complex superimposition of numerous factors controlling segmentation and subsidence within graben.
5. Throw on graben faults reaches 15 m, being lower at fault ends and segment tips and increasing with segment length. The shape of throw profiles departs from elliptical being more irregular with increasing fault length. Deviations from the mean length/throw ratio for fault segments may have developed as a result of their linkage.
6. Normal faults have dilational components with the average opening of 2–5 m and the maximum located in the middle parts of most faults. The correlation between local opening and throw along faults is generally poor. Although boundaries of fault segments are distinguished both on throw and opening profiles, a significant shift between the maximum throw and opening is common for most segments. Local anomalies of asymmetrical throw and opening on faults across grabens suggest that, despite the general similarities in formation of graben faults, their segments propagate and link in a complex manner that involve a variety of structures largely affecting fault plane geometries.
7. A few orders of fault segmentation indicate that the present throw accumulated by many increments as faults underwent a series of changes in their geometry. Lateral propagation of fault segments occurs by means of new fractures that nucleate at their tips. Segments link by one or both tips propagating towards each other or by the development of intervening segments.

Acknowledgements

The authors would like to thank C. Talbot for discussions and for reviewing the manuscript.

References

Ackerman, R.V., Schlische, R.W., Withjack, M.O., 2001. The geometric and statistical evolution of normal fault systems: an experimental study of the effects of mechanical layer thickness on scaling laws. Journal of Structural Geology 23, 1803–1819.

Ackermann, R.V., Schlische, R.W., 1997. Anticlustering of small normal faults around larger faults. Geology 25, 1127–1130.

Acocella, V., Gudmundsson, A., Funiciello, R., 2000. Interaction and linkage of extension fractures and normal faults: examples from the rift zone of Iceland. Journal of Structural Geology 22, 1233–1246.

Angelier, J., Bergerat, R., Dauteuil, O., Villemin, T., 1997. Effective tension–shear relationships in extensional fissure swarms, axial rift zone of northeastern Iceland. Journal of Structural Geology 19, 673–685.

Bergerat, F., Angelier, J., Villemin, T., 1990. Fault systems and stress patterns on emerged oceanic ridges: a case study in Iceland. Tectonophysics 179, 183–197.

Bohnestiehl, D.R., Kleinrock, M.C., 2000. Evidence for spreading-rate dependence in the displacement–length ratios of abyssal hill faults at mid-ocean ridges. Geology 28, 395–398.

Carbotte, S.M., Macdonald, K., 1994. Comparison of seafloor tectonic fabric at intermediate, fast and superfast spreading ridges: influence of spreading rate, plate motions, and ridge segmentation on fault patterns. Journal of Geophysical Research 99, 13609–13631.

Carbotte, S.M., Mutter, J.C., Xu, L., 1997. Contribution of volcanism and tectonism to axial and flank morphology of the southern East pacific Rise, 17°10′–17°40′S, from a study of layer 2A geometry. Journal of Geophysical Research 102, 10165–10184.

Cartwright, J., Trudgill, B.D., Mansfield, C., 1995. Fault growth by segment linkage: an explanation for scatter in maximum displacement and trace length data from the Canyonlands grabens of SE Utah. Journal of Structural Geology 17, 1319–1326.

Cowie, P.A., 1998. Normal fault growth in three-dimensions in continental and oceanic crust. In: Buck, W.R., Delaney, P.T., Karson, J.A., Lagabrielle, Y. (Eds.), Faulting and Magmatism at Mid-Ocean Ridges. American Geophysical Union, Washington, pp. 325–348.

Cowie, P.A., Scholz, C.H., 1992. Displacement to length scaling relationships for faults: data synthesis and discussion. Journal of Structural Geology 14, 1149–1156.

Cowie, P.A., Malinverno, A., Ryan, W.B.F., Edwards, M.H., 1994. Quantitative fault studies on the East Pacific Rise: a comparison of sonar imaging techniques. Journal of Geophysical Research 99, 15205–15218.

Dawers, N.H., Anders, M.H., 1995. Displacement–length scaling and fault linkage. Journal of Structural Geology 17, 607–614.

Dawers, N.H., Anders, M.H., Scholz, C.H., 1993. Growth of normal faults: displacement–length scaling. Geology 21, 1107–1110.

Einarsson, P., 1991. Earthquakes and present-day tectonism in Iceland. Tectonophysics 189, 261–279.

Florenz, O.G., Gunnarsson, K., 1991. Seismic crustal structure in Iceland and surrounding area. Tectonophysics 189, 1–17.

Foulger, G.R., Jahn, C., Seeber, G., Einarsson, P., Julian, B., Heki, K., 1992. Post-rifting stress relaxation at the divergent plate boundary in northeast Iceland. Nature 358, 488–490.

Gawthorpe, R.L., Jackson, C.A.-L., Young, M.J., Sharp, I.R., Moustafa, A.R., Leppard, C.W., 2003. Normal fault growth, displacement localization and the evolution of normal fault populations: the Hammam Faraun fault block, Suez rift, Egypt. Journal of Structural Geology 25, 883–895.

Grant, J.V., Kattenhorn, S.A., 2004. Evolution of vertical faults at an extensional plate boundary, southwest Iceland. Journal of Structural Geology 23, 537–557.

Gudmundsson, A., 1987a. Geometry, formation and development of tectonic fractures on the Reykjanes Peninsula, southwest Iceland. Tectonophysics 139, 295–308.

Gudmundsson, A., 1987b. Tectonics of the Thingvellir fissure swarm, SW Iceland. Journal of Structural Geology 9, 61–69.

Gudmundsson, A., 2000. Dynamics of volcanic systems in Iceland: example of tectonism and volcanism at juxtaposed hot spot and mid-ocean ridge systems. Annual Review of Earth and Planetary Sciences 28, 107–140.

Gudmundsson, A., Bäckström, K., 1991. Structure and development of the Sveinagja graben, Northeast Iceland. Tectonophysics 200, 111–125.

Gupta, A., Scholz, C., 2000. Brittle strain regime transition in the Afar depression: implications for fault growth and seafloor spreading. Geology 28, 1087–1090.

Johannesson, H., Saemundsson, K., 1998. Geological map of Iceland. Tectonics, 1:500,000. Icelandic Institute of Natural History, Reykjavik.

Karson, J.A., 1998. Internal structure of oceanic lithosphere: a perspective from tectonic windows. In: Buck, W.R., Delaney, P.T., Karson, J.A., Lagabrielle, Y. (Eds.), Faulting and Magmatism at Mid-Ocean Ridges. American Geophysical Union, Washington, pp. 177–218.

Kattenhorn, S.A., Pollard, D.D., 2001. Integrating 3-D seismic data, field analyses, and mechanical models in the analyses of segmented normal faults in the Wytch Farm oil field, southern England, United Kingdom. AAPG Bulletin 85, 1183–1210.

Macdonald, K.C., 1998. Linkages between faulting, volcanism, hydrothermal activity and segmentation on fast spreading centres. In: Buck, W. R., Delaney, P.T., Karson, J.A., Lagabrielle, Y. (Eds.), Faulting and Magmatism at Mid-Ocean Ridges. American Geophysical Union, Washington, pp. 27–58.

Macdonald, K.C., Fox, P.J., Alexander, R.T., Pockalny, R., Gente, P., 1996. Volcanic growth faults and the origin of Pacific abyssal hills. Nature 380, 125–129.

Maerten, L., Willemse, E.J.M., Pollard, D.D., Rawnsley, K., 1999. Slip distributions on intersecting normal faults. Journal of Structural Geology 21, 259–271.

Mazzoli, S., Di Bucci, D., 2003. Critical displacement for normal fault nucleation from en-échelon vein arrays in limestones: a case study from the southern Apennines (Italy). Journal of Structural Geology 25, 1011–1020.

Muffler, L., Clynne, M., Champion, D.E., 1994. Late Quaternary normal faulting of the Hat Creek basalt, northern California. Geological Society of America Bulletin 106, 195–200.

Opheim, J.A., Gudmundsson, A., 1989. Formation and geometry of fractures and related volcanism of the Krafla fissure swarm, northeast Iceland. Geological Society of America Bulletin 101, 1608–1622.

Palmason, G., 1980. A continuum model of crustal generation in Iceland: kinematic aspects. Journal of Geophysics 47, 7–18.

Peacock, D.C.P., Parfitt, E.A., 2002. Active relay ramps and normal fault propagation on Kilauea Volcano, Hawaii. Journal of Structural Geology 24, 729–742.

Pollard, D.D., Segall, P., Delaney, P.T., 1982. Formation and interpretation of dilatant échelon cracks. Geological Society of America Bulletin 93, 1291–1303.

Rögnvaldsson, S.T., Gudmundsson, A., Slunga, R., 1998. Seismotectonic analysis of the Tjörnes Fracture Zone, an active transform fault in north Iceland. Journal of Geophysical Research 103 (B12), 30117–30129.

Rubin, A.M., Pollard, D.D., 1988. Dike-induced faulting in rift zones of Iceland and Afar. Geology 16, 413–417.

Saemundsson, K., 1977. Geological map of Iceland. Sheet 7, North East Iceland, 1: 250,000. First edition. The Iceland Geodetic Survey and the Museum of Natural History, Reykjavik.

Saemundsson, K., 1978. Fissure swarms and central volcanoes of the neovolcanic zones of Iceland. Geological Journal 10, 415–432.

Saunders, A.D., Fitton, J.G., Kerr, A.C., Norry, M.J., Kent, R.W., 1997. The North Atlantic Igneous Province. In: Mahoney, J.J., Coffin, M.F. (Eds.), Large Igneous Provinces: Continental, Oceanic and Planetary Geophysical Monograph. American Geophysical Union, Washington, DC, pp. 45–93.

Sigmundsson, F., Einarsson, P., Bilham, R., Sturkell, E., 1995. Rift-transform kinematics in south Iceland: deformation from Global Positioning System measurements, 1986 to 1992. Journal of Geophysical Research 100 (B4), 6235–6248.

Sigurdsson, H., Sparks, R.S.G., 1978. Rifting episode in north Iceland in 1874–1875 and the eruption of Askja and Sveinagja. Bulletin Volcanologique 41, 149–167.

Smallwood, J.R., Staples, R.K., Richardson, K.R., White, R.S., 1999. Crust generated above the Iceland mantle plume; from continental rift to oceanic spreading center. Journal of Geophysical Research 104, 22885–22902.

Tentler, T., 2003a. Analogue modeling of tension fracture pattern in relation to mid-ocean ridge propagation. Geophysical Research Letters 30, 11–14.

Tentler, T., 2003b. Analogue modeling of overlapping spreading centers: insights into their propagation and coalescence. Tectonophysics 376, 99–115.

Tentler, T., Temperley, S., 2003. Segment linkage during evolution of intracontinental rift systems: insights from analogue modelling. In: Nieuwland, D. (Ed.), New Insights into Structural Interpretation and Modelling Geological Society, London, Special Publications, 212, pp. 181–196.

Thayer, R.E., Björnsson, A., Alvarez, L., Hermance, J.F., 1981. Magma genesis and crustal spreading in the northern neovolcanic zone of Iceland: telluric–magnetotelluric constraints. Geophysical Journal of Royal Astronomical Society 65, 423–442.

Thorarinsson, S., 1959. Some geological problems involved in the hydro-electric development of the Jökulsa a Fjöllum, Iceland. Report to the State Electricity Authority, Reykjavik.

Tucholke, B.E., Lin, J., 1994. A geological model for the structure of ridge segments in slow-spreading crust. Journal of Geophysical Research 99, 11937–11958.

Walsh, J.J., Watterson, J., 1987. Distribution of cumulative displacement and of seismic slip on a single normal fault surface. Journal of Structural Geology 9, 1039–1046.

Walsh, J.J., Bailey, W.R., Childs, C., Nicol, A., Bonson, C.G., 2003. Formation of segmented normal faults: a 3-D perspective. Journal of Structural Geology 25, 1251–1262.

Watterson, J., Walsh, J.J., Gillespie, P.A., Easton, S., 1996. Scaling systematics of fault sizes on a large-scale range fault map. Journal of Structural Geology 18, 199–214.

Wilkins, S.J., Gross, M.R., 2002. Normal fault growth in layered rocks at Split Mountain, Utah: influence of mechanical stratigraphy on dip linkage, fault restriction and fault scaling. Journal of Structural Geology 24, 1413–1429.

Willemse, E.J., 1997. Segmented normal faults: correspondence between three dimensional mechanical models and field data. Journal of Geophysical Research 102, 675–692.